

## Efficiency of a Compound Parabolic Collector for Domestic Hot Water Production using the F - Chart Method

Kevin Ortega Quispe<sup>1,2</sup>, Oscar Huari Vila<sup>3</sup>, Dennis Ccopi Trucios<sup>1,2</sup>, Arlitt Lozano Povis<sup>1</sup>, Lucia Enriquez Pinedo<sup>1,2</sup> and Betty Cordova Torres<sup>2,\*</sup>

<sup>1</sup>Facultad de Ciencias Forestales y del Ambiente, Universidad Nacional del Centro del Perú, Av. Mariscal Castilla N° 3089, 12002 Huancayo, Perú

<sup>2</sup>Dirección de Desarrollo Tecnológico Agrario, Estación Experimental Agraria Santa Ana, Instituto Nacional de Innovación Agraria (INIA), Carretera Saños Grande-Hualahoyo Km 8 Santa Ana, Huancayo, Jumin 12002, Perú

<sup>3</sup>Facultad de Ingeniería Mecánica, Universidad Nacional del Centro del Perú, Av. Mariscal Castilla N° 3089, 12002 Huancayo, Perú

Received 13 December 2023; Accepted 23 May 2024

### Abstract

Among solar energy technologies, differences exist in terms of costs, performance, and environmental sustainability. Flat-plate solar collectors, solar towers, and parabolic dish systems offer high thermal efficiency and versatility, but they may be more costly and bulky compared to other collector models. This study focused on evaluating the efficiency of a cylindrical parabolic collector (CPC) for the production of domestic hot water in a high Andean region of Peru, using the F-Chart method. Its performance was estimated considering the energy demand for hot water in a single-family home with four occupants, in accordance with national regulations and international recommendations. Additionally, the collector area, water temperature, and incident solar radiation were determined based on meteorological data obtained using the PVsyst software. On the other hand, the F-Chart methodology was employed to find the dimensionless factors X and Y of the CPC collector, which allowed estimating the solar fraction factor and the monthly useful energy that can be provided by the designed CPC system. The results showed that, during months of maximum solar radiation, the CPC is capable of satisfying between 129% and 144% of the energy demand for hot water. This indicates that there is a surplus of usable solar energy in the collector during the summer, while in autumn and winter, the solar contribution balances and slightly exceeds the demand. CPC can significantly contribute to the development of high Andean areas by improving quality of life, reducing costs, and promoting environmental sustainability compared to other available technologies.

*Keywords:* Efficiency, Thermal Performance, Domestic Hot Water, Solar Radiation, Thermal Modeling

### 1. Introduction

In recent years, population development has been driven by the use of conventional energies, which pose a significant threat to the sustainability of the planet, the quality of life for people, and future generations [1-2]. Furthermore, it is known that due to industrial development and the increase in the world population, energy demand has significantly risen, resulting in negative impacts on the environment and limiting the availability of the planet's finite resources [3-4]. As a consequence, renewable energies and other sustainable options are gaining unprecedented importance to meet the growing energy needs of the population. This momentum is promoting by the objective of mitigating the effects of climate change [5]. Well, they are more accessible, generate fewer emissions than fossil fuels, and other non-renewable sources [3]. Among these, solar energy emerges as a viable option since it provides an inexhaustible energy source and does not cause harm to the environment [6-9].

On the other hand, the need to produce domestic hot water is among the areas or sectors that require special attention to reduce energy consumption [10]. Currently, conventional water heating systems rely on electricity and/or fossil fuels, which have proven to be extremely energy-inefficient, exacerbating the issue by

generating highly detrimental emissions to the environment and having a negative impact on the economy of the population [11]. Therefore, cylindrical parabolic collectors (CPC) have emerged as a promising and emerging alternative for obtaining domestic hot water due to their high thermal efficiency and design that allows them to capture and concentrate incident radiation with minimal emissions of harmful gases [12-14]. On the other hand, flat solar collector systems, solar towers and parabolic dishes offer high thermal efficiency and versatility due to their ability to effectively capture and concentrate solar radiation into thermal energy.

However, this efficiency and versatility can come with higher costs and greater bulk [15]. In non-concentrating solar thermal collectors, the surface area of the collector is equal to the area of the absorber. In contrast, in concentrating solar thermal collectors, the collector surface is larger than the absorption region [16]. Vacuum tube collectors (ETC) and flat plate collectors (FPC) are the main types of commercial non-concentrating collectors available on the market. Working fluid temperatures can vary between 303 and 423 K, depending on the collector system [17]. In concentrating solar collectors, mirrors, reflectors, or solar trackers are used to direct solar radiation from the collector area to the absorption region. Concentrating collectors operate with working fluids that reach significantly higher temperatures than non-concentrating collectors [18].

\*E-mail address: 46754383@continental.edu.pe

ISSN: 1791-2377 © 2024 School of Science, DUTH. All rights reserved.

doi:10.25103/jestr.173.17

Regarding this topic, several researchers have studied the issues and focused on the study of the structure of CPCs for the production of domestic hot water. They have also suggested various techniques and methods to improve their performance [13]. However, while there is still much to discover in this field, these authors agree that the use of CPCs has positioned itself as a very promising alternative for the production of domestic hot water, taking advantage of the abundant available solar energy [14] as is the case in the Andean region of Peru, with an average of 5.3 kWh/m<sup>2</sup> per day [19].

Thus, the F-Chart method emerges as a structured and efficient system for thermal solar systems [20-22]. This approach is based on conducting an energy balance, which allows estimating the fraction of total heating load that will be provided by solar energy for a heating system such as a CPC. In turn, it enables a precise and detailed assessment of the collector's performance according to critical parameters affecting its efficiency. Moreover, it accurately calculates the amount of heat that can be captured and transferred, considering important factors such as incident solar radiation, ambient temperature, and water temperature [23].

The objective of this research is to assess the efficiency of a cylindrical parabolic collector (CPC) using the F-Chart method, based on estimating the average behavior of thermal solar systems in relation to the demand for domestic hot water in a high Andean region and a single-person household. Additionally, this research aims to contribute to the achievement of various Sustainable Development Goals (SDGs), including SDG 3 for health and well-being by promoting clean energies that do not cause air pollution; SDG 7 for affordable and clean energy by fostering renewable sources; SDG 11 for sustainable cities and communities by encouraging low-carbon technologies; and SDG 6 for clean water and sanitation by proposing sustainable options that do not compromise water resources. In this way, progress can be made in various targets and indicators of the mentioned SDGs, supporting the transition towards an inclusive, reliable, and environmentally sustainable energy model for the country, with both environmental and social benefits [24-25].

## 2. Materials and Methods

### 2.1 Location

The current study was conducted in the city of Huancayo, located in the central Andean region of Peru (12.0°S, 75.3°W). With an average of 5.3 kWh/m<sup>2</sup> per day [19], the city is an ideal location for solar energy utilization due to its high direct radiation throughout most of the year. The CPC prototype was installed on the rooftop of a building in the city center at an approximate altitude of 3,266 meters above sea level. This location in the central Andes provides ideal conditions of radiation and dry climate for the implementation of such technologies [26]. Additionally, the system is supplied with drinking water from the city's distribution network, and both measurements and system tests were conducted throughout the twelve months of the year 2022.

### 2.2 Cylindrical Parabolic Collector

The parabolic shape is common in many energy concentrators because this design has the ability to reflect sunlight in parallel towards its axis, concentrating the rays at its focus with the same intensity along its walls [27]. The CPC prototype used in this study has been constructed by applying the equation of a parabola, where the equation is determined

by the quadratic expression  $F(x) = x^2/80$ . The values assigned to  $X$  correspond to the area of the reflective surface (stainless steel metal sheet). It is important to note that the directrix of the function is  $Y - P = 0$ , perpendicular to the focal axis.

In Fig. 1, the reference points for bending the sheet are illustrated. It is worth noting that each value taken by the variable  $X$  will determine the walls of the concentrator.

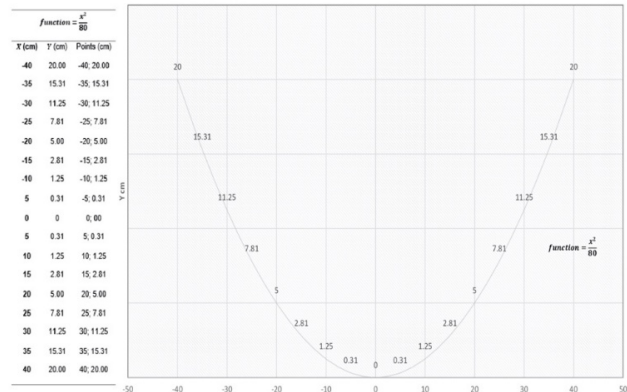


Fig. 1. Points of Reference for Sheet Bending

For the construction of the CPC prototype (Fig.2), a 240 x 140 cm, 3 mm thick stainless-steel sheet was used. The supporting metal structure was crafted using 3/8" corrugated iron, 3/8" cylindrical bar, and 1 1/2" square tube for the uprights. The parabolic movement of the system, generating its directionality, was achieved using 6205-2RS series bearings. The absorber consisted of a 1" inch and 240 cm long copper tube, positioned 20 cm from the reflective sheet, coinciding with the focus of the parabola. Hydraulic connections utilized 1" PVC fittings, two 1/2" ball valves, two 1" to 1/2" galvanized reducers, two 3/4" to 1/2" galvanized unions, and a 10-meter hose.

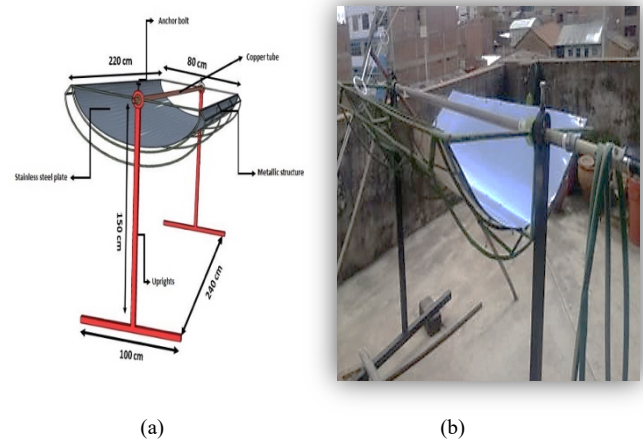


Fig. 2. Model CPC side view (a), prototype CPC to scale and actual size (b).

The system relied on the principle of reflecting sunlight towards a common focal point to harness solar energy [3]. The parabolic surface reflected the incident radiation towards the focal point, where a copper receiver tube was positioned. The focal point of the parabola served as the placement location for this tube. As a result, the reflected sunlight was concentrated on the tube, reaching the necessary temperature to heat the sanitary water that flowed through the copper tube. The design and construction of the prototype achieved a capacity of 1.76 m<sup>2</sup> for the reception area of solar light.

With respect to the calibration of the prototype, it was performed at the National University of Central Peru (UNCP) through a standard 0 to 100°C thermometer, Nicety digital thermometer model DT 811, which exhibits a measurement range of -10 to 250°Celsius. This calibration procedure was conducted prior to each measurement or experimental operation involving the equipment.

### 2.3. F-Chart Method

This method provided an estimation of the fraction of the total heating load supplied by solar energy to the system [28], through the value of  $f$ , which corresponds to the fraction of the monthly heating load (hot water) provided by solar energy as a function of two dimensionless parameters.  $X$  (collector loss) represented the ratio between collector losses and heating loads, while  $Y$  (collector gain) represented the ratio between absorbed solar radiation and heating loads [23], [29].

In order to determine the dimensionless loss variable  $X$ , the following equation was utilized:

$$X = F_R U_L * \left(\frac{F'_R}{F_R}\right) * (T_{ref} - T_a) * \Delta t * \frac{Ac}{L} \quad (1)$$

From this equation,  $F_R$  which is the heat exchanger efficiency factor of the collector,  $U_L$ , the overall loss coefficient of the collector typically expressed in  $\left(\frac{w}{m^2} \text{ } ^\circ C\right)$ , the total number of seconds in a month denoted as  $\Delta t$ , another variable  $T_a$ , the average monthly ambient temperature ( $^\circ C$ ),  $T_{ref}$ , the empirical reference temperature ( $100^\circ C$ ),  $\left(\frac{F'_R}{F_R}\right)$  the collector heat exchanger correction factor (0.97),  $A_C$ , the collector area ( $m^2$ ), and  $L$ , the total monthly heating load ( $GJ$ ), could be extracted. On the other hand, the incident solar variable was represented by the gain variable  $Y$ , given in Equation 2.

$$Y = F_R (\tau\alpha)_n * \left(\frac{F'_R}{F_R}\right) * \frac{(\tau\alpha)}{(\tau\alpha)_n} * H_T * N * \frac{Ac}{L} \quad (2)$$

Where  $(\tau\alpha)_n$  was evaluated as the average monthly transmittance product of absorbance, and  $\frac{(\tau\alpha)}{(\tau\alpha)_n}$  as the ratio between the transmittance and the average monthly incident absorbance (0.96). Regarding  $N$ , it represented the number of days in the month,  $H_T$  the monthly average of daily incident radiation on the collector surface per unit area shown in ( $J/m^2$ ). Next, to determine  $L$  (total monthly heating load for hot water), Equation3 will be used.

$$L = p * 75 * c_p * (T_w - T_m) * N \quad (3)$$

Where  $p$  is the number of beneficiaries. So, once the values of  $X$  and  $Y$  are obtained,  $f$  (monthly fraction of the load satisfied by solar energy) was estimated, deduced from Equation4. It is worth noting that if the formula yields a value of  $c$  less than 0, the value of 0 is used, but if  $F$  is greater than 1, the value of 1 is used.

$$f = 1.029Y - 0.065X_c - 0.245Y^2 + 0.0018X_c^2 + 0.0215Y^3 \quad (4)$$

On the other hand, the fraction  $F$  is a representation of the performance of the thermal solar system. This annual heating load supplied by solar energy was the sum of the monthly contributions of solar energy divided by the annual load, as shown in Equation 5.

$$F = \frac{\sum_{i=1}^{12} f_i L_i}{\sum_{i=1}^{12} L_i} \quad (5)$$

### 2.4. Domestic Hot Water Requirement

To assess the efficiency of the CPC, the domestic hot water requirement for a single-family dwelling with four occupants was determined following ISO Standard 010 [30] and OMS guidelines. The allocation must meet consumption needs at a minimum temperature of 60°C, ensuring the elimination of bacteria such as *Legionella pneumophila*, commonly found in water supply systems. Hot water should cover all hygiene and cleaning needs. The calculated allocation was 40 L/day, corresponding to four residents [31]. The thermal demand for hot domestic water corresponded to Equation 6.

$$D_{ACS} = Q_{ACS(T_{ref})} * \rho * C_p * (T_{ref} - T_{af}) * N \quad (6)$$

Meanwhile, the monthly thermal demand was calculated based on the daily consumption of domestic hot water at a reference temperature ( $Q_{ACS(T_{ref})}$ ), which is a crucial value to generate to avoid oversizing the CPC. Also, the density of water ( $\rho$ ) is required, which is 1 kg/l, and the specific heat ( $C_p$ ) is equivalent to 4.187 J/kg °C. Regarding temperatures, the cold water transported by the water supply systems' distribution network ( $T_{ref}$ ) and the reference water temperature ( $T_{af}$ ) both measured in °C, are needed. Finally,  $N$  represents the number of days in the month.

On the other hand, the energy demand for the volume of domestic hot water was calculated using Equation7.

$$E = m * C_p * (T_{ACS} - T_{af}) = m * C_p * \Delta t \quad (7)$$

Where  $E$  represents the energy demanded by the domestic hot water installation expressed in kWh,  $m$  is the mass of the hot water in kg/liter,  $C_p$  is the specific heat of water, and  $\Delta t$  is the temperature variation between the average temperature of the domestic hot water service and the temperature of the cold water or water from the network supply (15°C).

### 2.5. Monthly Incident Solar Radiation

Solar radiation consists of three components: direct beam, diffuse, and reflected radiation. In this context, the F-chart method is employed to identify an optimal tilt angle that maximizes the solar radiation reaching a collector with a collection area of 1.76 m<sup>2</sup>. To achieve this, the average radiation for each month is taken into account. In the event that the radiation data is provided on a daily basis, it is necessary to calculate a monthly average [32].

The models for obtaining radiation values are diverse, such as the empirical Bristow Campbell model, which utilizes monthly average temperatures or data from meteorological stations [33]. Additionally, the data was compared and adjusted using the PVsyst software due to its capability to calculate daily solar radiation values based on monthly data from sources like NASA-SSE and Meteonorm. Moreover, this software incorporates a comprehensive global meteorological database from ground stations, including irradiance, temperature, and wind speed [19]. It also provides tools for optimization, design, and simulation of solar systems. Another key advantage is that it generates detailed solar trajectory information for the specific project site.

## 3. Results and Discussion

Table 1 synthesizes the compilation of essential data for calculating the domestic hot water requirement, considering a single-family dwelling occupied by four individuals, as detailed in Equation 6, 7, and specified for each month of the year 2022, based on a collection area of 1.76 m<sup>2</sup>. The table also includes the calculation of the monthly energy demand for domestic hot water in a residence, according to the

regulations and recommendations mentioned earlier. Factors such as daily consumption per person, population, required water temperature, and other relevant parameters were taken into account. The analysis reveals a total annual energy requirement of 872.62 kWh to meet the domestic hot water needs of the dwelling based on its characteristics and location.

**Table 1.** Monthly Energy Demand Requirement

Year 2022	Conv. Factor	Service T° demand	Days Month	Cp (kJ/kg°C)	Indicated T° (°C)	Service T° (°C)	Tap Water T° (°C)	Energy Demand (kWh/mth)
Jan	1.38	34.62	31	4.187	60	45	6	77.88
Feb	1.39	34.87	28	4.187	60	45	7	69.04
Mar	1.42	35.42	31	4.187	60	45	9	73.55
Apr	1.44	36.03	30	4.187	60	45	11	68.39
May	1.45	36.36	31	4.187	60	45	12	69.23
June	1.47	36.72	30	4.187	60	45	13	65.60
July	1.48	37.10	31	4.187	60	45	14	66.34
Aug	1.47	36.72	31	4.187	60	45	13	67.78
Sept	1.45	36.36	30	4.187	60	45	12	66.99
Oct	1.44	36.03	31	4.187	60	45	11	70.67
Nov	1.42	35.42	30	4.187	60	45	9	71.18
Dec	1.38	34.62	31	4.187	60	45	6	77.88
<b>Total</b>								<b>872.62</b>

\*Daily demand = 40 L

The monthly variation of incident solar radiation on the collector plane, as shown in Table 2, provides essential information for estimating exploitable thermal energy. It is evident that higher radiation values will be recorded during the spring and summer months, while lower levels occur in the fall and winter months, following a characteristic seasonality pattern. Additionally, these fluctuations will

directly influence the energy that the CPC receiver can capture during each season of the year.

Furthermore, correction factors for solar radiation were necessary to estimate factor X, according to Equation 1. This dimensionless factor is a crucial input that represents the relationship between collector losses and heating loads.

**Table 2.** Energy to be captured by the monthly CPC

Year 2022	Hasr (kWh/m <sup>2</sup> ·day)	Correction factor K	Casr (kWh/m <sup>2</sup> ·day)	Absorbed energy (kWh/ Month)	Demand (kWh/ Month)	X
Jan	4.59	1.39	6.38	292.93	77.88	3.76
Feb	4.80	1.29	6.19	256.79	69.04	3.72
Mar	4.56	1.16	5.29	242.87	73.55	3.30
Apr	5.59	1.04	5.81	258.31	68.39	3.78
May	5.65	0.95	5.37	246.44	69.23	3.56
June	5.98	0.92	5.50	244.45	65.60	3.73
July	6.45	0.95	6.13	281.34	66.34	4.24
Aug	6.42	1.05	6.74	309.50	67.78	4.57
Sept	5.31	1.21	6.43	285.48	66.99	4.26
Oct	5.64	1.39	7.84	359.95	70.67	5.09
Nov	5.67	1.50	8.51	377.90	71.18	5.31
Dec	4.82	1.48	7.13	327.53	77.88	4.21

\*Horizontal average solar radiation = Hasr; Corrected average solar radiation = Casr

In Table 3, the dimensionless factors Y corresponding to solar gain were obtained from Equation 2 using the F-Chart method. It is observed that the Y factor varies throughout the year in accordance with changes in solar radiation. In contrast, the X factor depends primarily on ambient and water temperatures, resulting in a less variable behavior.

May	12	14.1	0.91	6.41
June	13	18.8	0.88	5.96
July	14	22.5	0.86	5.69
Aug	13	22	0.82	5.34
Sept	12	18.6	0.83	5.56
Oct	11	12.8	0.89	6.21
Nov	9	7.5	0.89	6.32
Dec	6	4.5	0.81	5.63

**Table 3.** Solar profit by monthly CPC

Year 2022	Tap Water Temperature (°C)	Ambient temperature (°C)	K2	Y
Jan	6	4.3	0.81	5.67
Feb	7	5.5	0.84	5.86
Mar	9	8	0.88	6.23
Apr	11	10.3	0.93	6.68

Table 4 presents the calculation of the solar fraction or factor f obtained from Equation 4, representing the proportion of the monthly energy demand that can be covered by the CPC collector, based on the previously determined values of the dimensionless variables X and Y. It is observed that during the months with maximum solar radiation, corresponding to

the summer season, the  $f$  factor exceeds unity, reaching values from 1.29 to 1.44. This indicates that in these months, there is a surplus of solar energy available that can be utilized by the CPC in relation to the demand for domestic hot water.

It is interesting to discuss how the system behaves in other regions with different solar radiation. In a study by Frauberth et al. [19], conducted in Malaysia, the reported values for the  $f$  factor ranged between 0.70 and 0.92, which is lower than the value obtained in our case. Although the capture area of the reflector in this study was larger at 2 m<sup>2</sup> compared to our prototype of 1.76 m<sup>2</sup>, the radiation levels in Malaysia were significantly lower, with an average of 4 kWh/m<sup>2</sup>-day compared to our 5.3 kWh/m<sup>2</sup>-day in our high-altitude zone. Herefore, to assess the adaptability and renewable capacity of the CPC system, it is necessary to consider not only the relationship between solar radiation and the capture area but also other parameters and meteorological conditions. Additionally, adjustments over time can result in optimized system performance, as supported by Afzanizam et al. [23]. This comparative analysis suggests that the proposed CPC system offers good performance and opens the possibility of adaptation to areas with varied solar energy resources, provided proper prototype sizing, consideration of climatic characteristics, and detailed analysis of radiation for each region are undertaken.

In a similar scenario, during the coldest months of winter, the  $f$  factor manages to reach unity, with values between 1.17 and 1.28. This indicates that the solar fraction provided by the CPC is still sufficient to meet 100% of the energy demand for a single-family home in the high-altitude zones during those months.

By contrasting the calculated demand with the monthly useful energy supplied by the CPC collector, it is confirmed that a surplus of energy is obtained during the summer, while in the fall and winter, solar contribution is just enough to cover the demand. Consequently, an auxiliary system is required to complement the CPC contribution during the colder months of the year, allowing it to operate smoothly.

**Table 4.** Monthly usable useful energy

Year 2022	X	Y	$f$	Demand (kWh/month)	Useful Energy (kWh/month)
Jan	3.76	5.67	1.24	77.88	96.39
Feb	3.72	5.86	1.23	69.04	84.59
Mar	3.30	6.23	1.17	73.55	85.71
Apr	3.78	6.68	1.20	68.39	81.80
May	3.56	6.41	1.19	69.23	82.06
June	3.73	5.96	1.22	65.60	80.12
July	4.24	5.69	1.29	66.34	85.31
Aug	4.57	5.34	1.34	67.78	90.93
Sept	4.26	5.56	1.29	66.99	86.69
Oct	5.09	6.21	1.39	70.67	98.35
Nov	5.31	6.32	1.44	71.18	102.19
Dec	4.21	5.63	1.28	77.88	100.03

In Figure 3, the monthly energy demand for domestic hot water, calculated, is visually compared with the useful energy provided by a CPC solar collector through a 1.76 m<sup>2</sup> collection panel. It is evident that during the hot summer months (December to March), the energy supplied by the CPC significantly exceeds the energy demand, suggesting that surplus solar energy can be utilized for other basic needs. On the other hand, during the fall and winter (April to August), solar contribution approximately balances with the

demand, covering the demand without creating a pronounced surplus.

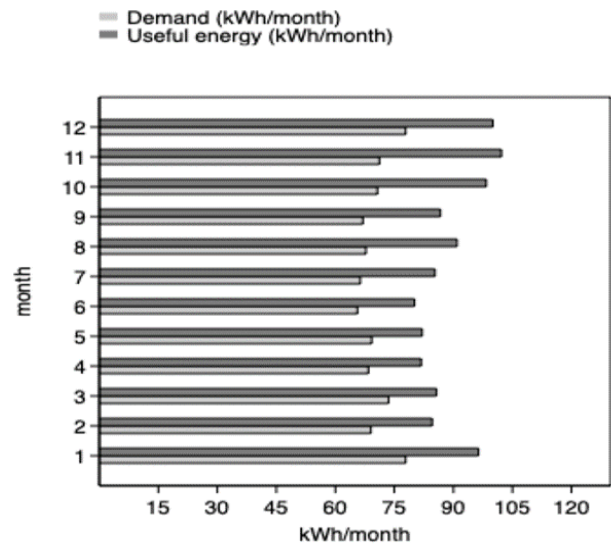


**Fig. 3.** Covered demand for domestic hot water

Therefore, a properly sized CPC collector has the capacity to provide the required power and generation of domestic hot water throughout the year, even during months of higher energy demand. It is important to note the efficiency of the CPC model compared to other solar collectors in this context. The study by Kocer and Ertekin [28] compares the performance of a CPC collector against a flat-plate collector under the meteorological conditions of Turkey. The results report higher monthly  $f$  factor values for the CPC, reaching 0.9 in the summer months, whereas the flat-plate collector only achieves 0.7. Similarly, the useful energy provided by the CPC is higher throughout the year, especially during the winter months, where it nearly doubles the generation of the flat-plate system.

During the study of the cylindrical parabolic collector (CPC) in the Peruvian Andes, several challenges and limitations were identified. Seasonal variations, cloud cover, and solar radiation affected its performance, particularly in autumn and winter [34-35]. The accuracy of meteorological data and proper sizing of the collector are crucial to avoid evaluation errors and power issues. Additionally, the initial installation and maintenance costs require a long-term profitability analysis. Special conditions in high Andean regions, such as altitude and low temperatures, also influence efficiency of the CPC [18].

CPCs can be efficiently adapted to various geographical conditions with minimal efficiency losses and are viable for large district heating systems. Additionally, CPCs are suitable for producing heat at high temperatures with low heat losses, unlike flat plate collectors [36]. In high-altitude regions, the use of high thermal efficiency materials is crucial due to low temperatures. In cloudy areas, it is recommended to combine the CPC with alternative energy sources and solar tracking systems. Furthermore, the CPC can be adapted to different scales, from single-family homes to industrial applications, benefiting from economies of scale and potential government incentives [37].

The implementation of thermal solar energy systems such as parabolic trough collectors on a larger scale poses various significant economic challenges. It is essential to carefully evaluate the cost of electricity and the overall project value.

Although they may be viable in various high-radiation regions, highly optimized systems are necessary to ensure profitability. Therefore, specific studies considering local climatic and economic conditions are required [38-39].

Regarding the scalability and economic viability of the technology, the compound parabolic collector (CPC) can be utilized at the industrial level in thermal power plants. Additionally, it could be employed on a large scale in all the highland regions of Peru for the generation of sanitary hot water, as a means to reduce the high mortality rates in children and elderly people due to annual low temperatures (frijajes). Although other models exist that could perform the same function [40-43], the model under study presents greater viability from an economic standpoint, since the materials used for its construction are accessible anywhere and are low-cost. Likewise, the construction process can be carried out in any metal-mechanic workshop with basic equipment and specialized labor.

This demonstrates that, under different geographic and climatic conditions, the CPC collector exhibits better efficiency and thermal performance compared to conventional flat-plate technologies. Therefore, the proposed CPC model in this study would also have performance advantages over alternatives, making it a promising option for solar water heating in high-radiation areas.

#### 4. Conclusions

The analysis conducted using the F-Chart method allowed for a detailed description of the thermal performance of a CPC, estimating its instantaneous performance under actual conditions at the research location. The simulation results indicate that the CPC can meet between 117% and 144% of the monthly energy demand for domestic hot water in a four-person single-family home in a high-altitude region. This suggests that during the months of peak solar radiation, corresponding to the summer, the CPC will have an excess of thermal energy, and there will be a balance between demand and available useful energy during the winter months. These surpluses can be utilized to supplement other domestic energy needs, such as heating or similar requirements, which are crucial in these high-altitude areas where low temperatures are common. Additionally, the applied approach

verified the technical feasibility of the CPC system for the proposed residential application throughout the year, as the solar energy proportion would be balanced and even exceed the demand for hot water.

Therefore, this study extends the potential use of the F-Chart method to model and optimize concentration thermal solar systems in regions of Latin America with high levels of solar radiation or other areas with similar meteorological conditions. The results obtained lay the groundwork for the design and implementation of larger-scale CPC systems in urban areas or rural communities in the Andean region, aiming to bridge gaps and achieve sustainable development goals.

Based on the results of our CPC prototype, it is recommended to investigate the use of advanced materials with enhanced thermal properties for key components of the CPC, such as reflectors and the thermal receiver. This could include the use of selective coatings to improve solar radiation absorption and reduce thermal losses, as well as the use of materials with high thermal conductivity to enhance heat transfer within the system. Economic and environmental feasibility studies are recommended for future research to assess cost-benefit in different contexts and application scenarios.

This would help inform investment decisions and policies related to the adoption and promotion of CPC as a viable and sustainable renewable energy technology. These recommendations could provide promising areas for future research and improvements in CPC design, with the aim of maximizing its performance and its contribution to the use of clean and sustainable energy in the high Andean regions and beyond.

#### Acknowledgments

A heartfelt gratitude goes to the Faculty of Environmental Engineering at Continental University and the Faculty of Mechanical Engineering at the National University of Central Peru for generously providing access to equipment and research facilities.

This is an Open Access article distributed under the terms of the Creative Commons Attribution License.



#### References

- [1] A. Ullah, Q. Zhang, S. Raza, and S. Ali, "Renewable energy: Is it a global challenge or opportunity? Focusing on different income level countries through Panel Smooth Transition Regression Model," *Renew. Ener.*, vol. 177, pp. 689–699, Nov. 2021.
- [2] J. P. Delong, O. Burger, and M. J. Hamilton, "Current Demographics Suggest Future Energy Supplies Will Be Inadequate to Slow Human Population Growth," *PLoS One*, vol. 5, no. 10, pp. 13206–13226, 2010.
- [3] A. Pinedo and D. Asmat, "Análisis teórico-experimental del colector solar cilíndrico parabólico automatizado con espejos reflectantes," *Rev. Enc. Cient. Intern.*, vol. 7, no. 2, Feb. 2010.
- [4] S. Ram, H. Ganesan, V. Saini, and A. Kumar, "Performance assessment of a parabolic trough solar collector using nanofluid and water based on direct absorption," *Renew Ener.*, vol. 214, pp. 11–22, Sep. 2023.
- [5] R. Salim, K. Hassan, and S. Shafiei, "Renewable and non-renewable energy consumption and economic activities: Further evidence from OECD countries," *Ener. Econ.*, vol. 44, pp. 350–360, Jul. 2014.
- [6] A. Lee, H. Kang, C. Lin, and K. Shen, "An integrated decision-making model for the location of a PV solar plant," *Sustainability (Switzerland)*, vol. 7, no. 10, pp. 13522–13541, 2015.
- [7] N. Souidi, S. Nanayakkara, N. Jahed, and S. Naahidi, "Rise of nature-inspired solar photovoltaic energy converters," *Sol. Ener.*, vol. 208, no. 1, pp. 31–45, Sep. 2020.
- [8] W. Pickard, "A simple lower bound on the EROI of photovoltaic electricity generation," *Ener. Pol.*, vol. 107, pp. 488–490, Aug. 2017.
- [9] B. Sahu, "Solar energy developments, policies and future prospectus in the state of Odisha, India," *Renew. Sustain. Ener. Rev.*, vol. 61, pp. 526–536, Aug. 2016.
- [10] A. Heidari, N. Olsen, P. Mermod, A. Alahi, and D. Khovalyg, "Adaptive hot water production based on Supervised Learning," *Sustain. Cities Soc.*, vol. 66, pp. 102625–102638, Mar. 2021.
- [11] W. Liu *et al.*, "Environmental life cycle assessment and techno-economic analysis of domestic hot water systems in China," *Ener. Convers Manag.*, 199, pp. 111943–111954, Nov. 2019.
- [12] İ. Yılmaz and A. Mwesigye, "Modeling, simulation and performance analysis of parabolic trough solar collectors: A comprehensive review," *Appl. Ener.*, vol. 225, pp. 135–174, Sep. 2018.
- [13] V. K. Jebasingh and G. M. Herbert, "A review of solar parabolic trough collector," *Renew. Sustain. Ener. Rev.*, vol. 54, pp. 1085–1091, Feb. 2016.
- [14] A. Abdulhamed, N. Adam, M. Ab-Kadir, and A. Hairuddin, "Review of solar parabolic-trough collector geometrical and thermal analyses,

- performance, and applications,” *Renew. Sustain. Ener. Rev.*, vol. 91, pp. 822–831, Aug. 2018.
- [15] Y. Asaad, I. Seres, and I. Farkas, “Experimental investigation of parabolic trough solar collector thermal efficiency enhanced with different absorber coatings,” *Int. J. Thermofl.*, vol. 19, p. 100386, Aug. 2023.
- [16] L. Li, B. Wang, J. Pye, and W. Lipinski, “Concentrating collector systems for high-temperature solar thermal applications,” *OSA Adv. Photon. Cong. 2021*, Jul. 2021.
- [17] J. Qin, E. Hu, G. J. Nathan, and L. Chen, “Concentrating or non-concentrating solar collectors for solar Aided Power Generation?” *Ener. Convers. Manag.*, vol. 152, pp. 281–290, Nov. 2017.
- [18] I. Wole-oshon, E. Okonkwo, S. Abbasoglu, and D. Kavaz, “Nanofluids in Solar Thermal Collectors: Review and Limitations,” *Int. J. Thermophys.*, vol. 41, no. 11, Nov. 2020.
- [19] B. Frauberth, C. Lapa, J. Raúl, and M. Hernández, “Desarrollo del modelo bristow campbell para estimar la radiación solar global de la región de junin, Perú,” *Tecnol. Quim.*, vol. 35, no. 2, pp. 220–234, 2015.
- [20] E. Cavalcanti, “Analisis of Experimental Solar Radiation Data For Rio De Janeiro, Brazil,” *Solar Ener.*, vol. 47, no. 3, pp. 231–235, 1991.
- [21] J. E. Braun, S. A. Klein, and K. A. Pearson, “An Improved Desing Method for Solar Water Heating Systems,” *Solar Ener.*, vol. 31, no. 6, pp. 597–604, 1983.
- [22] S. Kalogirou, “Modeling and Design of Solar Energy Systems Including Solar Economics,” *Solar Energy Conversion and Photoenergy Systems*, 2008.
- [23] M. Afzanizam *et al.*, “F-Chart Method for Design Domestic Hot Water Heating System in Ayer Keroh Melaka,” *J. Adv. Res. Fluid Mechanic. Ther. Sci. J.*, vol. 56, no. 1, pp. 59–67, 2019.
- [24] S. Saint, A. Alola, A. Akadiri, and U. Alola, “Renewable energy consumption in EU-28 countries: Policy toward pollution mitigation and economic sustainability,” *Ener. Polic.*, vol. 132, pp. 803–810, Sep. 2019.
- [25] L. Yiu and R. Saner, “Sustainable Development Goals and Millennium Development Goals: an analysis of the shaping and negotiation process,” *Asian Pacif. J. Public Administr.*, vol. 36, no. 2, pp. 89–107, May 2014.
- [26] L. Suárez, J. Flores, A. Pereira, and H. Karam, “Ultraviolet solar radiation in the tropical central Andes (12.0°S),” *Photochem. Photobiolog. Sci.*, vol. 16, no. 6, pp. 954–971, 2017.
- [27] L. Saravia, “Diseño gráfico de concentradores tipo CPC,” *Energ. Renov. Medio Amb.*, vol. 8, no. 1, Jan. 2004.
- [28] A. Kocer and C. Ertekin, “A Comparison of Flat Plate and Evacuated Tube Solar Collectors with F-Chart Method,” *J. Therm. Sci. Techn.*, vol. 35, no. 1, pp. 77–86, 2015.
- [29] J. Haberl and P. Soolyeon, “Literature Review of Uncertainty of Analysis Methods,” Texas A&M University, Texas, USA, ESL-TR-04/11-01, Nov. 2004. [Online]. Available: <https://oaktrust.library.tamu.edu/bitstream/handle/1969.1/2072/ESL-TR-04-11-01.pdf?sequence=1&isAllowed=y>
- [30] MVCS and SENCICO, “Reglamento Nacional de Edificaciones - DS 011- 2006-Vivienda,” Lima, 2006.
- [31] Guías técnicas sobre saneamiento, agua y salud, Cantidad mínima de agua necesaria para uso doméstico., OMS, EE.UU., 2009.
- [32] F. Do Rego, A. Gatto, S. Alves, and M. da Fonseca, “Program for Solar Water Heating Systems Based on the F-Chart Method,” *J. Mech. Engin. Autom.*, vol. 4, no. 9, pp. 752–762, 2014.
- [33] B. Camayo, J. Pomachagua, J. Massipe, M. Quispe, and A. Torres, “Validation and application of Bristow Campbell model for estimating the global solar radiation in the Junin region,” *Tecnol. Quim.*, vol. 37, no. 3, 2017.
- [34] F. Canaza, “Efecto de las variaciones climáticas y atmosféricas en el rendimiento energético de los paneles solares monofaciales, Chachapoyas, Amazonas,” *Rev. Cient. Pakamuros*, vol. 10, no. 3, pp. 64–77, Sep. 2022.
- [35] A. Marín, A. Gómez, R. Román, A. Marín, A. Gómez, and R. Román, “Variación estacional de la temperatura media y los flujos advectivos y atmosféricos de calor en un embalse tropical andino,” *Rev. Acad. Colomb. Cienc. Exactas Fis. Nat.*, vol. 44, no. 171, pp. 360–375, Jun. 2020.
- [36] A. R. Jensen and I. Sifnaios, “Modeling, Validation, and Analysis of a Concentrating Solar Collector Field Integrated with a District Heating Network,” *Solar*, vol. 2, no. 2, pp. 234–250, May 2022.
- [37] D. Panaroni, L. Martorelli, and A. C. Luna, “Análisis y evaluación de la eficiencia coseno de un colector cilindro parabólico polar: Aplicación en una región subtropical de Argentina,” *ACI Avan. Cienc. Ingen.*, vol. 13, no. 2, pp. 15–15, Nov. 2021.
- [38] A. John and J. Oyekale, “Techno-economic feasibility analysis of a large- scale parabolic trough thermal power plant in Effurun-Warri, Nigeria,” *Int. J. Ener. Smart Grid*, vol. 8, no. 1, pp. 1–11, Jan. 2023.
- [39] M. E. Lopes *et al.*, “Technical-economic feasibility analysis of a large- scale parabolic trough collectors solar power plant in Brazil,” *RE&PQJ*, vol. 21, no. 3, pp. 337–344, Jul. 2023.
- [40] H. Saeed *et al.*, “Performance Evaluation of an Evacuated Flat-Plate Collector System for Domestic Hot Water Applications,” *J. Sol. Ener. Eng.*, vol. 145, no. 5, pp. 51006–51018, Oct. 2023.
- [41] M. Kashan, A. Fung, and J. Swift, “Integrating Novel Microchannel-Based Solar Collectors with a Water-to-Water Heat Pump for Cold-Climate Domestic Hot Water Supply, Including Related Solar Systems Comparisons,” *Energies (Basel)*, vol. 14, no. 13, pp. 4057–4064, Jul. 2021.
- [42] A. Oltarzewska and D. Krawczyk, “The Use of Solar Collectors in Domestic Hot Water Systems in Central and Eastern European Countries: Simulation in TRNSYS,” *Environm. Clim. Technol.*, vol. 27, no. 1, pp. 243–253, Jan. 2023.
- [43] S. Pathak, V. V. Tyagi, K. Chopra, A. K. Pandey, and A. Sari, “Hot Water Generation for Domestic Use in Residential Buildings via PCM Integrated U-Tube Based Solar Thermal Collector: A 4-E Analysis,” *Buildings*, vol. 13, no. 5, pp. 1212–1220, May. 2023.